Supplement of Atmos. Chem. Phys., 15, 10925–10938, 2015
http://www.atmos-chem-phys.net/15/10925/2015/
doi:10.5194/acp-15-10925-2015-supplement

Atmospheric Chemistry and Physics Open Access

Supplement of

Influence of synoptic patterns on surface ozone variability over the eastern United States from 1980 to 2012

L. Shen et al.

Correspondence to: L. Shen (lshen@fas.harvard.edu)

1 Spatial patterns of temporal variability in daily JJA surface ozone in the eastern United States in different site types

Here we examine whether the bimodal structure of observed ozone variability is sensitive to the type of EPA-AQS site (rural, suburban, and urban). Fig. S1 shows the zonally averaged ozone concentrations, standard deviation (SD), and relative SD for the three site types across the eastern United States for different time intervals. As in Fig. 1, we include in our analysis all sites reporting at least one observation every summer during 1980-2012, resulting in 787 rural, 617 suburban, and 266 urban sites altogether. Zonally averaged ozone concentrations at all site types reveal a unimodal structure peaking around 35°N-40°N for all time spans, with an overall trend of decreasing concentrations from 1980 to present. The absolute ozone SD shows a bimodal structure for all time spans at rural sites, with peaks at 29°-35°N and 39°-43°N. At urban and suburban sites, the northern peak in absolute SD diminishes over time, while the southern peak persists, consistent with the more rapid NOx reductions in the North (Russell et al., 2012). In contrast, the relative ozone SD shows a clear bimodal structure for all three site types and all time intervals. Our finding that the bimodal structure is a robust feature in both the absolute and relative ozone SD at rural sites thus reflects the smaller influence of anthropogenic emissions at such sites. In calculating the relative SD, we remove much of the influence of anthropogenic emissions. The persistent bimodal structure of the relative SD in ozone across time and sites therefore gives us confidence that the relative SD can be used to identify those regions where meteorology plays a large role in driving ozone variability.

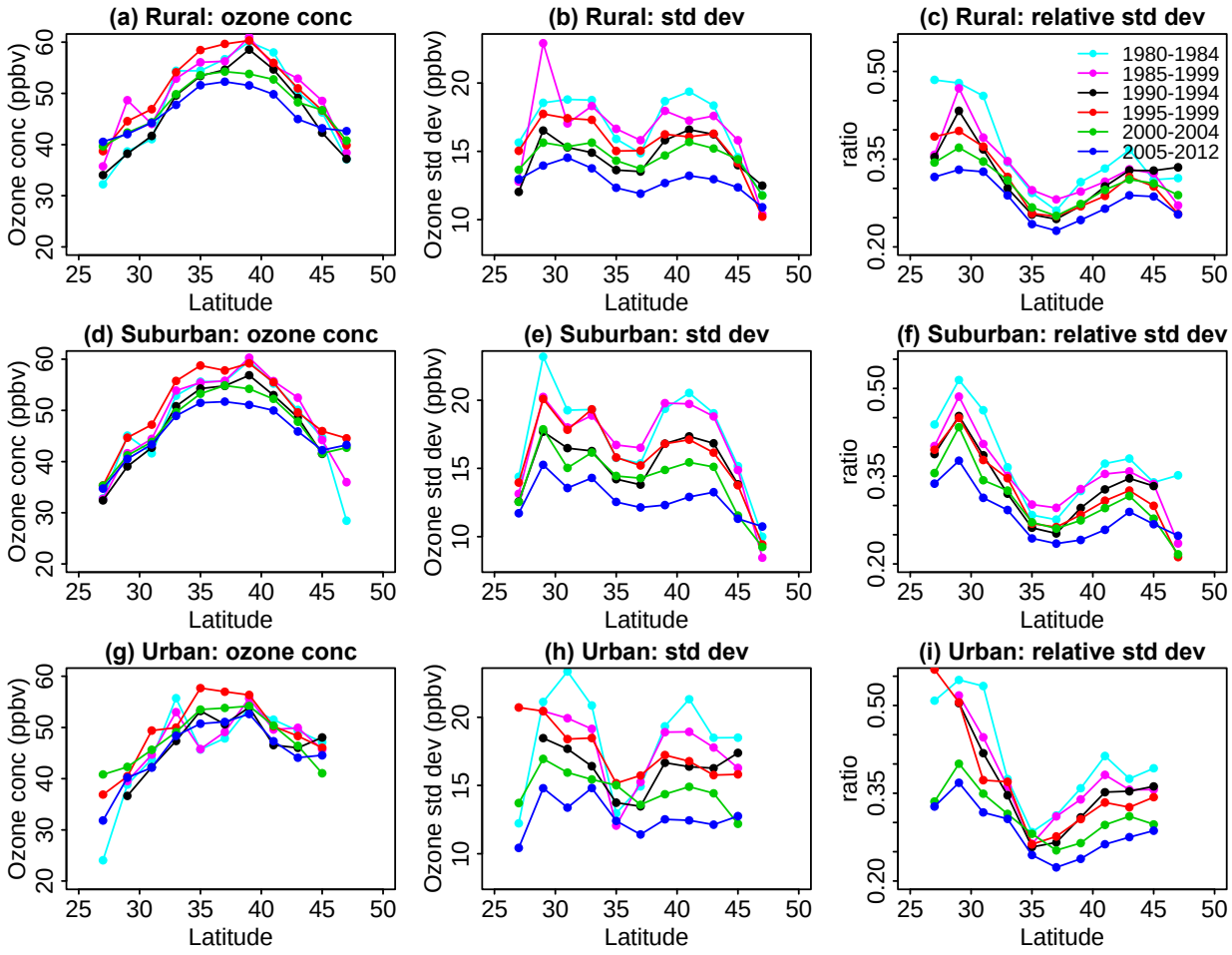

Figure S1. Latitudinal variation of zonal mean ozone concentrations (a, d, g), ozone standard deviation (b, e, h), and relative standard deviation (c, f, i). All values are for JJA mean MDA8 ozone. The top row shows results from rural sites, the middle from suburban sites, and the bottom from urban sites in AQS. Data have been averaged between 100°W and 65°W longitude and binned to 2° intervals in latitude. The different colors denote different 5-year time intervals, except for the most recent interval, which is 8 years in length.

2 Correlation of ozone and Great Plains low level jet (GPLLJ)

Here we seek to examine more closely the causes for the pattern in the third empirical orthogonal function (EOF3) of daily JJA maximum daily 8-hour average (MDA8) ozone over the eastern United States. To that end, we calculate the correlation of JJA MDA8 ozone and the GPLLJ wind speed, which we define as the daily mean meridional wind speed at 850 hPa averaged over a 10°×5° box in the southern part of the Great Plains (26.25°-36.25°N, 101.25°-96.25°W) as indicated by the red rectangle in Fig. S2. This region corresponds to the core of the GPLLJ (Zhu

and Liang, 2013). We follow the approach of Zhu and Liang (2013) but use daily data instead of monthly data since our focus is on the daily variability. Figure S2 shows the relationship of daily detrended and deseasonalized MDA8 ozone concentration and the GPLLJ wind speed, with negative correlations in the South Central and positive correlations in the Great Lakes and East coast regions. Our result is similar to that of Zhu and Liang (2013) but with much lower correlations due to the finer temporal resolution. The figure shows that a strong GPLLJ ventilates Texas and the central United States, but is associated with slightly increased ozone in the Northeast and Southeast.

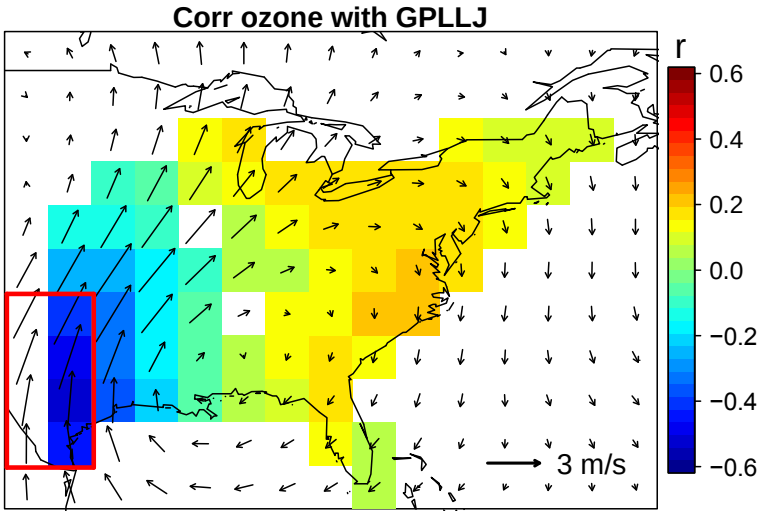

Figure S2. Correlations (in color) of the 1980-2012 timeseries of daily JJA MDA8 ozone anomalies across the United States and the daily meridional wind speeds at 850 hPa averaged over the region indicated by the red rectangle. Ozone values have been detrended and deseasonalized. Black arrows denote the composite 850 hPa wind anomalies on days when the meridional windspeed within the red rectangle is greater than the JJA median GPLLJ over this time period (6.4 m s^{-1}).

3 Use of empirical orthogonal functions to diagnose drivers of seasonal JJA ozone variability

We repeat the EOF analysis using the timeseries of 1980-2012 JJA mean ozone fields, instead of daily mean fields. In using daily data, the first three EOFs explain just 53% of the total variance in ozone; here we find that using seasonal mean data can explain 75% of the total variance. This is because the averaging process from daily to seasonal data can smooth noisy data. Figure S3 shows the results of this EOF analysis and the correlations of the PCs with different

meteorological variables. The top three EOF patterns are similar to those we derive using daily mean ozone (Fig. 3), but with one slight difference, as detailed below. We first describe the similarities between the two EOF analyses. Like EOF1 derived from daily ozone data (Fig. 3a), EOF1 here is linked to the north-south movement of the polar jet (Fig. S3a-3c) and explains 48% of the total variance in seasonal JJA ozone. The next two EOFs derived from seasonal data are similar to the next two derived from daily data, but with the order reversed. Like EOF3 with daily ozone data (Fig. 3g), EOF2 here exhibits an east-west pattern characteristic of a westward extension of Bermuda High and an enhanced GPLLJ (Fig. S3d-3f). This EOF explains 15% of the total variance. Finally, like EOF2 with daily ozone data (Fig. 3d), EOF3 here displays a northeast-southwest pattern associated with enhanced 850 hPa meridional wind from the Gulf of Mexico (Fig. S3g and 3h). This EOF explains 11% of the total variance. The key difference between the two EOF analyses can be seen by comparing Fig. 3f and S3i: in the seasonal EOF analysis, the link between EOF3 and 850 hPa geopotential height is much weaker than what we find using daily ozone data. This weak relationship makes clear that the analysis using seasonal ozone data fails to identify the influence of Bermuda High west edge on ozone air quality. As we discuss in Sect. 6, the failure arises because the influence of the Bermuda High on ozone varies nonlinearly with the location of the Bermuda High west edge, and the monthly mean EOF analysis obscures this nonlinear relationship. Because the daily dataset provides a greater abundance of observations, the EOF analysis using these data can identify the fine structure of ozone variability.

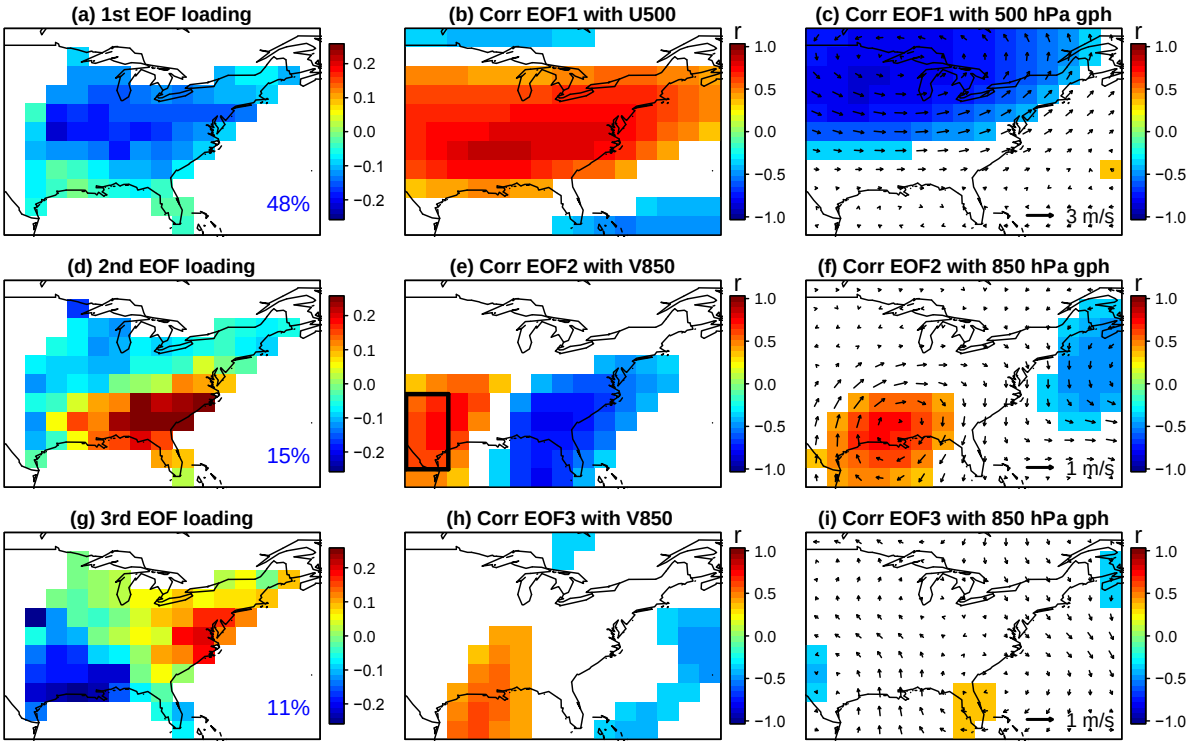

Figure S3. The top panels show (a) the spatial loadings of the first EOF pattern (EOF1) in JJA mean surface MDA8 ozone over the United States from 1980 to 2012 and the correlations *r* between the principal components time series for the first mode (PC1) and (b) JJA mean 500 hPa zonal wind speeds and (c) 500 hPa geopotential height. Composite 500 hPa wind anomalies associated with positive PC1 are shown as black arrows in Panel (c). Panel (d) is same as (a), but for the second EOF pattern (EOF2). Also shown are the correlations between PC2 and (e) JJA mean 850 hPa meridional wind speed and (f) JJA mean 850 hPa geopotential height. The composite 850 hPa wind anomalies with positive PC2 are shown as black arrows in Panel (f). Panel (g) is same as (a), but for the third EOF pattern (EOF3). Correlations are shown between PC3 and (h) 850 hPa meridional wind speeds and (i) 850 hPa geopotential heights. Panel (i) also shows the composite 850 hPa wind anomalies associated with positive PC3 (black arrows). White areas in all panels indicate either missing data or grid boxes where the correlation is not significant at the 0.05 level.

4 Definition of Bermuda High west edge

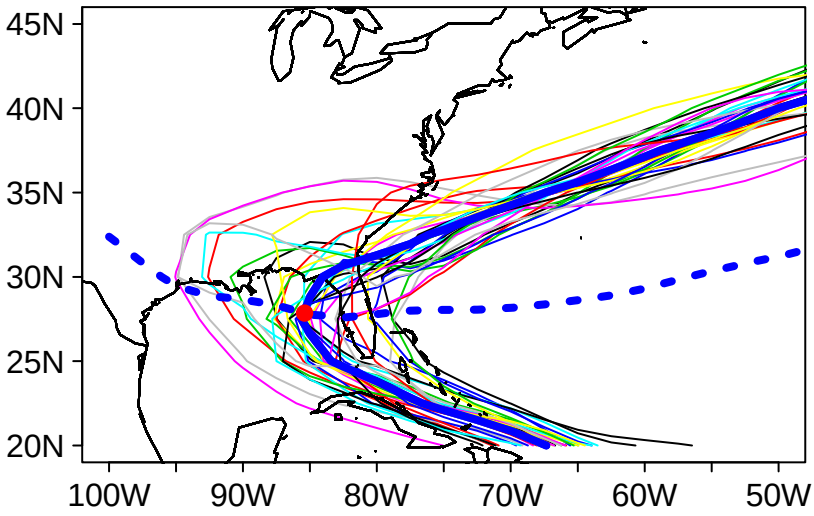

Figure S4. The definition of Bermuda High west edge. The bold blue solid curve denotes the climatological 1560-gpm isoline in June-July-August (JJA) from 1980 to 2012. The dashed curve line is the climatological u = 0 ms^{-1} ridge line at 850 hPa for the same time period. The intersection point, as denoted by the red points, is defined as the Bermuda High west edge, as in Li et al. (2011). The thin solid curves represent the mean JJA 1560-gpm isolines in different years from 1980 to 2012. The geopotential heights shown in this figure have been adjusted, as described in Sect. 6.

5 Linear trend of sea level pressure (SLP) from 1980 to 2012

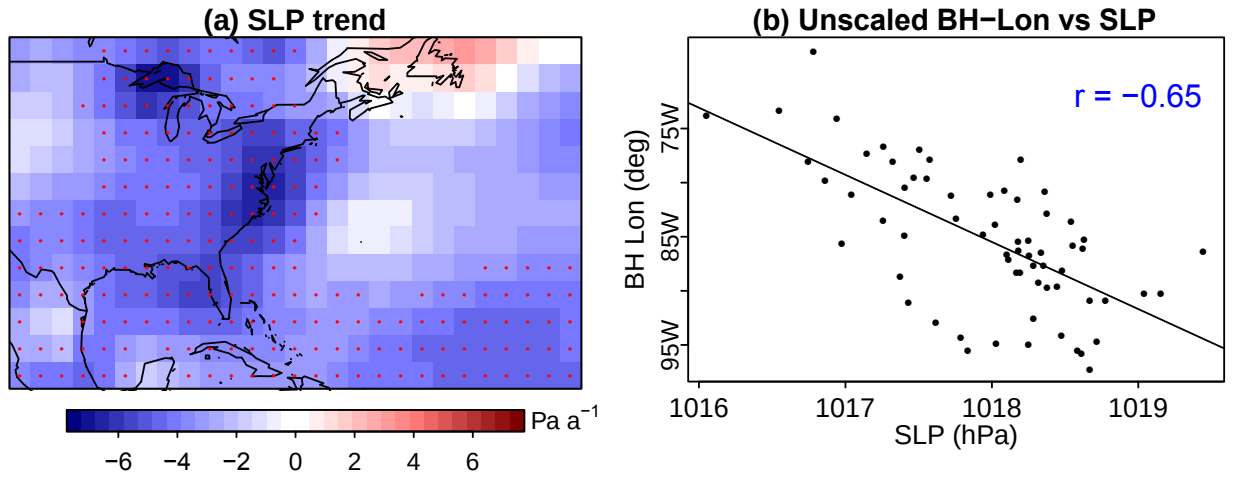

Figure S5. (a) The linear trend (Pa a^{-1}) of mean JJA sea level pressure (SLP) over much of North America and the North Atlantic. Red dots indicate gridboxes where the trend is significant ($p \leq 0.05$). (b) Relationship of the longitude of the Bermuda High west edge (unscaled BH-Lon) as defined by Li et al. (2011) and mean JJA SLP averaged over the Bermuda High domain (100°W~40°W, 20°N~40°N) during the 1948-2012 timeframe. Each point represents one summer. The correlation coefficient *r* is shown inset.

6 Variation of the standard deviation of BH-Lon as a function of the isoline of geopotential height

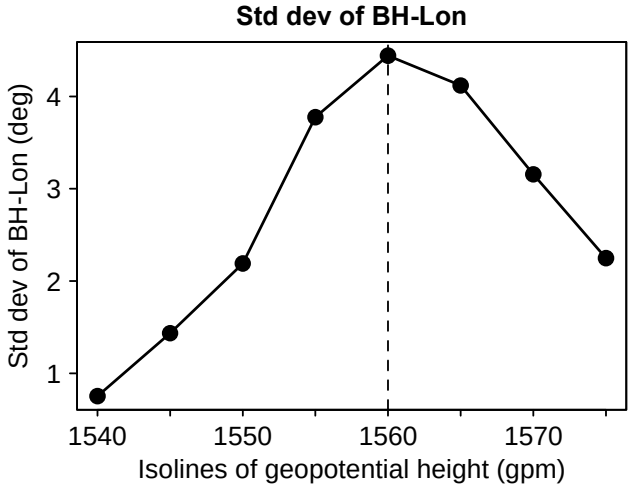

Figure S6. Standard deviation over the 1980-2012 time period of the mean JJA longitudes of the Bermuda High west edge, as defined by different isolines of the geopotential height at 850 hPa. The plot shows BH-Lon adjusted for the uniform changes in geopotential height, as described in Sect. 6.

7 Correlation of ozone and locations of Bermuda High west edges

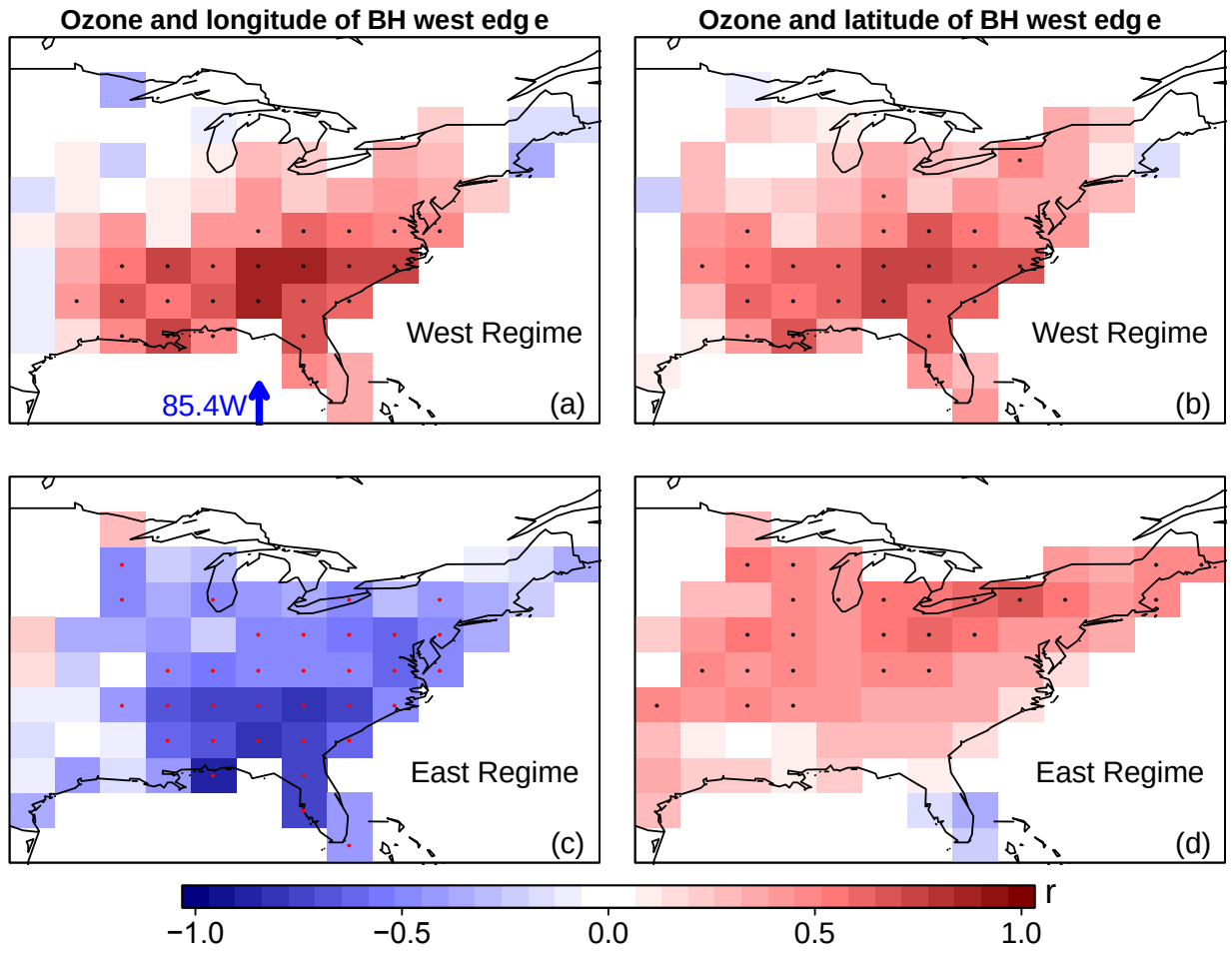

Figure S7. Correlations of the mean JJA MDA8 ozone in the eastern United States and the location of the Bermuda High west edge over the 1980-2012 time period. Ozone concentrations have been detrended as described in text. Positive values indicate increasing ozone with westward or northward shift of the longitude of the Bermuda High west edge. The top panels (a and b) show results for those summers when the west edge was located in the West Regime, with the 1560-gpm crossing the 850 hPa wind ridge line west of 85.4°W. The bottom panels (c and d) show results for the East Regime, when the 1560-gpm BH-Lon crossed the 850 hPa wind ridge line east of 85.4°W. The location of 85.4°W is denoted by the blue arrow in Panel a. Red and black dots indicate those gridboxes where the slope is significant at the 0.10 level. For more details on the definition of the Bermuda High west edge for each regime, see text.